13

Dynamic Model, Control and Simulation of Cooperative Robots: A Case Study

Jorge Gudiño-Lau* & Marco A. Arteaga**
* *Facultad de Ingeniería Electromecánica*
Universidad de Colima
Mexico
** *Departamento de Control y Robótica*
División de Ingeniería Eléctrica, de la Facultad de Ingeniería
Universidad Nacional Autónoma de México
México

1. Introduction

The modelling and control of multiple robotic manipulators handling a constrained object requires more sophisticated techniques compared with a single robot working alone. Since the theory employed for cooperative robots is independent of their size, one can think of them as mechanical hands. The study of mechanical hands is important not only because these can be used as prosthetic devices for humans, but also because they increase considerably the manipulation capacity of a robot when substituting the usual gripper. Thus, robot hands (as well as cooperative robots), may find many areas of application nowadays. Many benefits can be obtained by using them in industrial manufacturing. A typical example is in a flexible assembly, where the robots join two parts into a product. Cooperative manipulators can also be used in material handling, *e.g.*, transporting objects beyond the load carrying capacity of a single robot. Furthermore, their employment allows to improve the quality of tasks in the manufacturer industry that require of great precision. On the other hand, cooperative robots are indispensable for skillful grasping and dexterous manipulation of objects. However, the literature about experimental results on the modeling, simulation and control of systems of multiple manipulators holding a common object is rather sparse.

A dynamic analysis for a system of multiple manipulators is presented in Orin and Oh (Orin & Oh 1981), where the formalism of Newton-Euler for open chain mechanisms is extended for closed chain systems. Another approach widely used is the Euler-Lagrange method (Naniwa *et al.* 1997). The equations of motion for each manipulator arm are developed in the Cartesian space and the impact of the closed chain is investigated when the held object is in contact with a rigid environment, for example the ground. Another general approach to obtain the dynamic model of a system of multiple robots is based on the estimation of the grasping matrix (Cole *et al.* 1992, Kuc *et al.* 1994, Liu *et al.* 2002, Murray *et al.* 1994, Yoshikawa & Zheng 1991). Here, the grasping matrix is used to couple the manipulators dynamics with that of the object, while this is

Source: Mobile Robots, Moving Intelligence, ISBN: 3-86611-284-X, Edited by Jonas Buchli, pp. 576, ARS/plV, Germany, December 2006

modeled by the Newton-Euler formulation. The dynamic analysis for cooperative robots with flexible joints holding a rigid object is presented in Jankowski *et al.* (Jankowski *et al.* 1993).

This work presents the study of the dynamic equations of a cooperative robot system holding a rigid object without friction. The test bed is made up of two industrial robots and it is at the Laboratory for Robotics of the National University of Mexico. The dynamic model for the manipulators is obtained independently from each other with the Lagrangian approach. Once the robots are holding the object, their joint variables are kinematically and dynamically coupled. Assuming that the coupling of the system is described by holonomic constraints, the manipulators and object equations of motion are combined to obtain the dynamic model of the whole system, which can be used for simulation purposes. It is important to stress that a robot manipulator in free motion does not have geometric constraints; therefore, the dynamic model is described by Ordinary Differential Equations (ODE). When working with constrained motion, the dynamic model is described by Differential Algebraic Equations (DAE). It is shown how the simulation of this kind of systems can be carried out, including a general approach to simulate contact forces by solving DAE's.

Early attempts to establish a relationship between the automatic control of robots carrying out a shared task are referred to Kathib's operational space formulation (Khatib 1987). During the 1980's, the most important research results considered the contact evolution during manipulation (Montana 1988). Such a contact evolution requires a perfect combination of position and force control. Some of the first approaches following this objective are presented in Ly and Sastry (Li & Sastry 1989) and Cole (Cole 1990). In those works, the dynamics of the object is considered explicitly. In Parra-Vega and Arimoto (Parra-Vega & Arimoto 1996), Liu *et al.* (Liu *et al.* 1997) and Parra-Vega *et al.* (Parra-Vega *et al.* 2001), control schemes which do not take into account the dynamics of the object but rather the motion constraints are designed. These control approaches have the advantage that they do not require an exact knowledge of the system model parameters, since an adaptive approach is introduced. More recently, Schlegl *et al.* (Schlegl *et al.* 2001) show some advances on hybrid (in terms of a combination of continuous and discrete systems) control approaches.

Despite the fact that Mason and Salisbury (Mason & Salisbury 1985) proposed the base of sensor-less manipulation in the 1980's, there are few control algorithms for cooperative robot systems which take into account the possible lack of velocity measurements. Perhaps because, since a digital computer is usually employed to implement a control law, a good approximation of the velocity vector can be obtained by means of numerical differentiation. However, recent experimental results have shown that a (digitalized) observer in a control law performs better (Arteaga & Kelly 2004). Thus, in Gudiño-Lau *et al.* (Gudiño-Lau *et al.* 2004) a decentralized control algorithm for cooperative manipulators (or robot hands) which achieves asymptotic stability of tracking of desired positions and forces by using an observer is given. In this work, a new control law based on a force filter is presented. This is a general control law, so that it can be applied to a system with more than two manipulators involved as well. The control scheme is of a decentralized architecture, so that the input torque for each robot is calculated in its own joint space and takes into account motion constraints rather than the held object dynamics. Also, an observer is employed to avoid velocity measurements and experimental results are presented to validate the theoretical results.

2. Experimental System

The system under study is made up of two industrial robots and it is at the Laboratory for Robotics of the National University of Mexico (Figure 1). They are the A465 and A255 of *CRS Robotics*. Even though the first one has six degrees of freedom and the second one five, only the first three joints of each manipulator are used in this case, while the rest of them are mechanically braked. Each joint is actuated by a direct current motor with optical encoders. Both manipulators have a crash protection device in the end effector and a force sensor installed on it; an aluminum finger is mounted on the sensor. The object is constituted by a melamine plastic box with dimensions 0.15m × 0.15m × 0.311m and weight 0.400kg. The experiments are performed in a Pentium IV to 1.4 GHz personal computer with two PCI-FlexMotion-6C boards of *National Instruments*. The sampling time is of 9ms. Controllers are programmed in the *LabWindows/CVI* software of *National Instruments*.

A schematic diagram of the robots holding an object is depicted in Figure 2. The system variables are the generalized coordinates, velocities, and accelerations, as well as the contact forces exerted by the end effector on the common rigid object, and the generalized input forces (*i.e.*, torques) acting on the joints.

Fig. 1. Robots A465 and A255 of CRS Robotics.

To describe the kinematic relationships between the robots and the object, a stationary coordinate frame C_0 attached to the ground serves as reference frame, as shown in Figure 2. An object coordinate frame C_2 is attached at the center of mass of the rigid object. The origin of the coordinate frame C_1 is located at the center of the end effector of robot A465. In the same way, the origin of the coordinate frame C_3 is located at the

center of the end effector of robot A255. The coordinate frame C_0 has been considered to be the inertial frame of the whole system. ${}^0\boldsymbol{p}_2$ is the position vector of the object center of mass expressed in the coordinate system C_0. ${}^0\boldsymbol{p}_1$ and ${}^0\boldsymbol{p}_3$ are vectors that describe the position of the contact points between the end effectors of robots A465, A255 and the object, respectively, expressed in the coordinate system C_0 (Gudiño-Lau & Arteaga 2005).

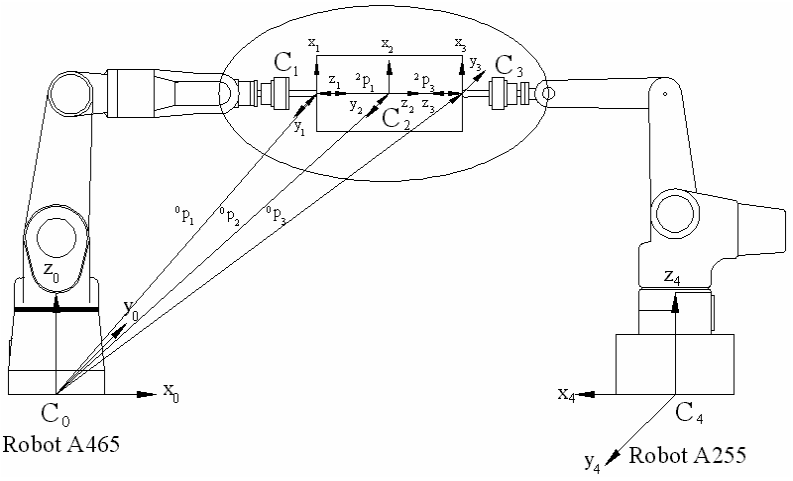

Fig. 2. Schematic diagram of robots holding an object.

3. The Cooperative Robots Dynamic Model

Consider the cooperative system with two robot arms shown in Figure 1, each of them with n_i =3 degrees of freedom and m_i=1 constraints arising from the contact with the held object. Then, the total number of degrees of freedom is given by $n=\sum_{i=1}^{2} n_i$ with a total number of $m=\sum_{i=1}^{2} m_i$ constraints.

3.1 Dynamic model with constraint motion and properties

The dynamic model for each individual manipulator, i=1,2, is obtained by the Lagrange's formulation as (Parra-Vega *et al.* 2001)

$$\boldsymbol{H}_i(\boldsymbol{q}_i)\ddot{\boldsymbol{q}}_i+\boldsymbol{C}_i(\boldsymbol{q}_i,\dot{\boldsymbol{q}}_i)\dot{\boldsymbol{q}}_i+\boldsymbol{D}_i\dot{\boldsymbol{q}}_i+\boldsymbol{g}_i(\boldsymbol{q}_i)=\boldsymbol{\tau}_i+\boldsymbol{J}_{\varphi_i}^{\mathrm{T}}(\boldsymbol{q}_i)\boldsymbol{\lambda}_i \tag{1}$$

where $\boldsymbol{q}_i\in\mathbb{R}^{n_i}$ is the vector of generalized joint coordinates, $\boldsymbol{H}_i(\boldsymbol{q}_i)\in\mathbb{R}^{n_i\times n_i}$ is the symmetric positive definite inertia matrix, $\boldsymbol{C}_i(\boldsymbol{q}_i,\dot{\boldsymbol{q}}_i)\dot{\boldsymbol{q}}_i\in\mathbb{R}^{n_i}$ is the vector of Coriolis and centrifugal torques, $\boldsymbol{g}_i(\boldsymbol{q}_i)\in\mathbb{R}^{n_i}$ is the vector of gravitational torques, $\boldsymbol{D}_i\in\mathbb{R}^{n_i\times n_i}$ is the positive semidefinite diagonal matrix accounting for joint viscous friction coefficients, $\boldsymbol{\tau}_i\in\mathbb{R}^{n_i}$ is the vector of generalized torques acting at the joints, and $\boldsymbol{\lambda}_i\in\mathbb{R}^{m_i}$ is the vector of Lagrange multipliers (physically represents the force applied at the contact point). $\boldsymbol{J}_{\varphi_i}^{\mathrm{T}}(\boldsymbol{q}_i)\boldsymbol{\lambda}_i$ represents the interaction of the rigid object with the two manipulators. $\boldsymbol{J}_{\varphi_i}(\boldsymbol{q}_i)=\nabla\boldsymbol{\varphi}_i(\boldsymbol{q}_i)\in\mathbb{R}^{m_i\times n_i}$ is assumed to be full rank in this paper. $\nabla\boldsymbol{\varphi}_i(\boldsymbol{q}_i)$ denotes the gradient of the object surface vector $\boldsymbol{\varphi}_i\in\mathbb{R}^{m_i}$, which maps a vector onto the normal plane at the tangent plane that arises at the contact point described by

$$\boldsymbol{\varphi}_i(\boldsymbol{q}_i) = 0\,. \tag{2}$$

Equation (2) is a geometrical constraint expressed in an analytical equation in which only position is involved and that does not depend explicitly of time *t*. Constraints of this forms are known as *holonomic constraints* (they are also classified as *sclero-holonomic*).

Note that equation (2) means that homogeneous constraints are being considered (Parra-Vega *et al.* 2001). The complete system is subjected to 2 holonomic constraints given by

$$\boldsymbol{\varphi}(\boldsymbol{q}) = 0\,, \tag{3}$$

where $\boldsymbol{\varphi}(q) = \boldsymbol{\varphi}(q_1, q_2) \in \mathbb{R}^{m_i}$. This means that the object being manipulated and the environment are modeled by the constraint (3). If the holonomic constraints are correctly calculated, then the object will remain hold.

Let us denote the largest (smallest) eigenvalue of a matrix by $\lambda_{\max}(\cdot)(\lambda_{\min}(\cdot))$. The norm of an $n\times 1$ vector x is defined by $\|\boldsymbol{x}\| \triangleq \sqrt{\boldsymbol{x}^T\boldsymbol{x}}$ while the norm of an $m\times n$ matrix $\boldsymbol{A}$ is the corresponding induced norm $\|A\| \triangleq \sqrt{\lambda_{\max}(A^T A)}$. By recalling that revolute joints are considered, the following properties can be established (Liu *et al.* 1997, Arteaga Pérez 1998, Parra-Vega *et al.* 2001):

Property 3.1. *Each* $\boldsymbol{H}_i(\boldsymbol{q}_i)$ *satisfies* $\lambda_{h_i}\|\boldsymbol{x}\|^2 \le \boldsymbol{x}^T\boldsymbol{H}_i(\boldsymbol{q}_i)\boldsymbol{x} \le \lambda_{H_i}\|\boldsymbol{x}\|^2 \quad \forall \boldsymbol{q}_i,\ \boldsymbol{x}\in\mathbb{R}^{n_i}$, *where* $\lambda_{h_i} \triangleq \min_{\forall \boldsymbol{q}_i\in\mathbb{R}^{n_i}} \lambda_{\min}(\boldsymbol{H}_i)$, $\lambda_{H_i} \triangleq \max_{\forall \boldsymbol{q}_i\in\mathbb{R}^{n_i}} \lambda_{\max}(\boldsymbol{H}_i)$ *and* $0 < \lambda_{h_i} \le \lambda_{H_i} < \infty$. Δ

Property 3.2. *With a proper definition of* $\boldsymbol{C}_i(\boldsymbol{q}_i, \dot{\boldsymbol{q}}_i)$, $\dot{\boldsymbol{H}}_i(\boldsymbol{q}_i) - 2\boldsymbol{C}_i(\boldsymbol{q}_i, \dot{\boldsymbol{q}}_i)$ *is skew-symmetric.* Δ

Property 3.3. *The vector* $\boldsymbol{C}_i(\boldsymbol{q}_i, \boldsymbol{x})\boldsymbol{y}$ *satisfies* $C_i(q_i, x)y = C_i(q_i, y)x \quad \forall x, y \in \mathbb{R}^{n_i}$. Δ

Property 3.4. *It is satisfied* $\|\boldsymbol{C}_i(\boldsymbol{q}_i, \boldsymbol{x})\| \le k_{ci}\|\boldsymbol{x}\|$ *with* $0 < k_{ci} < \infty, \forall \boldsymbol{x} \in \mathbb{R}^{n_i}$. Δ

Property 3.5. *The vector* $\dot{\boldsymbol{q}}_i$ *can be written as*

$$\begin{aligned} \dot{q}_i &= \dot{q}_i + \left(J_{\varphi_i}^+ J_{\varphi_i}\dot{q}_i - J_{\varphi_i}^+ J_{\varphi_i}\dot{q}_i\right) \\ &= \left(I_{n_i\times n_i} - J_{\varphi_i}^+ J_{\varphi_i}\right)\dot{q}_i + J_{\varphi_i}^+ J_{\varphi_i}\dot{q}_i \\ &\triangleq Q_i(q_i)\dot{q}_i + J_{\varphi_i}^+(q_i)\dot{p}_i\,, \end{aligned} \tag{4}$$

where $J_{\varphi_i}^+ = J_{\varphi_i}^T\left(J_{\varphi_i}J_{\varphi_i}^T\right)^{-1} \in \mathbb{R}^{n_i\times m_i}$ *stands for the Penrose's pseudoinverse and* $Q_i \in \mathbb{R}^{n_i\times n_i}$ *satisfies rank* $(Q_i) = n_i - m_i$. *These two matrices are orthogonal, i.e.* $Q_i J_{\varphi_i}^+ = 0$ *(and* $Q_i J_{\varphi_i}^T = 0$*).* $\dot{p}_i \triangleq J_{\varphi_i}\dot{q}_i \in \mathbb{R}^{m_i}$ *is the so called constrained velocity. Furthermore, in view of constraint (3), it holds*

$$\sum_{i=1}^{l}\dot{p}_i = 0 \quad \textit{and} \quad \sum_{i=1}^{l} p_i = \sum_{i=1}^{l}\int_0^t J_{\varphi i}\dot{q}_i \mathrm{d}\vartheta = 0\,. \tag{5}$$

Since homogeneous constraints are being considered, it also holds in view of (2) that

$$\dot{\boldsymbol{p}}_i = 0 \quad \textit{and} \quad \boldsymbol{p}_i = 0\,. \tag{6}$$

for i=1, . . . , l. $\boldsymbol{p}_i$ *is called the constrained position.* Δ

As shown in Liu *et al.* (Liu *et al.* 1997), if we consider homogeneous holonomic constraints we can write the constrained position, constrained velocity and constrained acceleration as

$$\boldsymbol{\varphi}_i(\boldsymbol{q}_i) = 0 \tag{7}$$

$$\dot{\boldsymbol{\varphi}}_i(\boldsymbol{q}_i) = \boldsymbol{J}_{\varphi i}(\boldsymbol{q}_i)\dot{\boldsymbol{q}}_i = 0 \tag{8}$$

$$\ddot{\boldsymbol{\varphi}}_i(\boldsymbol{q}_i) = \boldsymbol{J}_{\varphi i}(\boldsymbol{q}_i)\ddot{\boldsymbol{q}}_i + \dot{\boldsymbol{J}}_{\varphi i}(\boldsymbol{q}_i)\dot{\boldsymbol{q}}_i = 0, \tag{9}$$

respectively. Recall that in our case $n_i = 3$, $n = 6$, $m_i = 1$, and $m = 2$, i=1,2.

3.2 Dynamic model of the rigid object

The motion of the two robot arms is dynamically coupled by the generalized contact forces interacting through the common rigid object. To describe this interaction, it is necessary to know the object dynamics. According to the free body diagram of Figure 3, Newton's equation of motion are

$$\boldsymbol{m}_o\ddot{\boldsymbol{x}}_o - \boldsymbol{m}_o\boldsymbol{g}_o = \boldsymbol{f}_1 - \boldsymbol{f}_2, \tag{10}$$

where $\boldsymbol{m}_o \in \mathbb{R}^{3\times3}$ is the diagonal mass matrix of the object, $\ddot{\boldsymbol{x}}_o \in \mathbb{R}^3$ is the vector describing the translational acceleration of the center of mass of the rigid object, $\boldsymbol{f}_1 \in \mathbb{R}^3$ and $\boldsymbol{f}_2 \in \mathbb{R}^3$ are forces exerted by the robots, and $\boldsymbol{g}_o \in \mathbb{R}^3$ is a gravity vector. All vectors are expressed with reference to the inertial coordinate frame C_0. The contact forces vector are given by

$$\boldsymbol{f}_i = \boldsymbol{n}_i\lambda_i, \tag{11}$$

where $\boldsymbol{n}_i \in \mathbb{R}^3$ represents the direction of the force (normal to the constraint) and $\lambda_i \in \mathbb{R}$ given in (1).

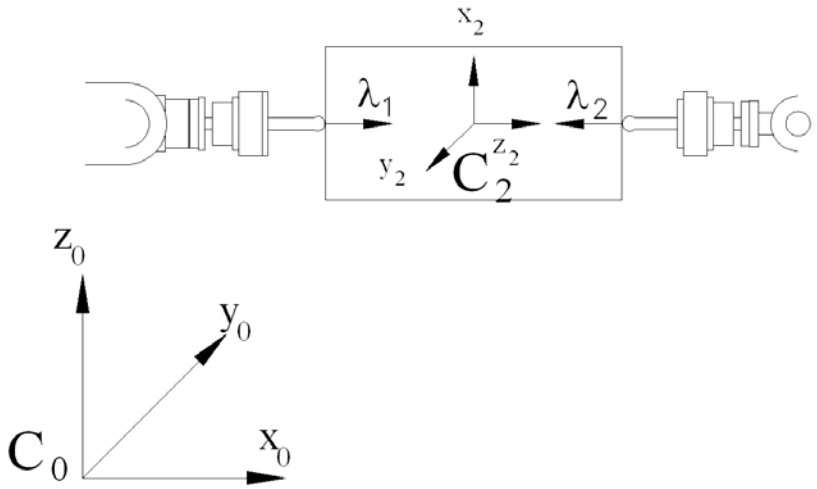

Fig. 3. Force free body diagram.

The following assumptions are made to obtain the dynamic model for the cooperative system and to design the control-observer scheme:

Assumption 3.1 *The end effectors (fingers) of the two robot arms are rigid.* Δ

Assumption 3.2 *The object is undeformable, and its absolute and relative position are known.* Δ

Assumption 3.3 *The kinematics of each robot is known* Δ

Assumption 3.4 *The l robots of which the system is made up satisfy constraints (2) and (6) for all time. Furthermore, none of the robots is redundant and they do not reach any singularity.* Δ

Assumption 3.5 *The matrix* $\boldsymbol{J}_{\varphi i}$ *is Lipschitz continuous, i. e.*

$$\left\|\boldsymbol{J}_{\varphi i}(\boldsymbol{q}_i) - \boldsymbol{J}_{\varphi i}(\boldsymbol{q}_{di})\right\| \le L_i\left\|\boldsymbol{q}_i - \boldsymbol{q}_{di}\right\|, \tag{12}$$

for a positive constant $\boldsymbol{L}_i$ *and for all* $\boldsymbol{q}_i, \boldsymbol{q}_{di} \in \mathbb{R}^{n_i}$. *Besides, there exist positive finite constants* c_{0i} *and* c_{1i} *which satisfies*

$$c_{0i} \triangleq \max_{\forall q_i \in \mathbb{R}^{n_i}} \left\| J_{\varphi i}^{+}(q_i) \right\| \tag{13}$$

$$c_{1i} \triangleq \max_{\forall q_i \in \mathbb{R}^{n_i}} \left\| J_{\varphi i}(q_i) \right\|' \tag{14}$$

Δ

Note that Assumption 3.4 is a common one in the field of cooperative robots. None of the robots can be redundant that (2) is satisfied only by a bounded vector q_i. On the other hand, the closed kinematic loop that arises when the manipulators are holding an object is redundant. Assumption 3.5 is quite reasonable for revolute robots, since the elements of q_i appear as argument of sines and cosines functions. This is why (13)-(14) is valid.

3.3 Dynamic coupling

The position, velocity and acceleration of the object center of mass with reference to the inertial coordinated frame are given in Cartesian coordinates by:

$$x_o = h_i(q_i) \tag{15}$$

$$\dot{x}_o = J_{oi}(q_i)\dot{q}_i \tag{16}$$

$$\ddot{x}_o = J_{oi}(q_i)\ddot{q}_i + \dot{J}_{oi}(q_i)\dot{q}_i\,, \tag{17}$$

respectively, with i = 1, 2. $h_i(q_i) \in \mathbb{R}^3$ is the forward kinematics of the center of mass of the object expressed in the coordinate system C_0, and $J_{oi}(q_i) \in \mathbb{R}^{3\times 3}$ is the corresponding Jacobian matrix of $h_i(q_i)$. Substituting (17) into (10) yields

$$m_o J_{oi}(q_i)\ddot{q}_i + m_o \dot{J}_{oi}(q_i)\dot{q}_i - m_o g_o = f_1 - f_2\,. \tag{18}$$

Now, consider writing (1) as (Murray *et. al* 1994)

$$H_i(q_i)\ddot{q}_i + C_i(q_i,\dot{q}_i)\dot{q}_i + D_i\dot{q}_i + g_i(q_i) = \tau_i + J_{ai}^{T}(q_i) f_i\,. \tag{19}$$

Note that

$$J_{\varphi i}^{T}(q_i) = J_{ai}^{T}(q_i) n_i\,, \tag{20}$$

in view of (11). $J_{ai}(q_i)$ is the manipulator analytical Jacobian. On the other hand, from (18) one gets

$$f_1 = m_o J_{oi}(q_i)\ddot{q}_i + m_o \dot{J}_{oi}(q_i)\dot{q}_i - m_o g_o + f_2\,. \tag{21}$$

Then, for i=1 in (19) one gets

$$\begin{aligned} &H_1(q_1)\ddot{q}_1 + C_1(q_1,\dot{q}_1)\dot{q}_1 + D_1\dot{q}_1 + g_1(q_1) = \\ &\tau_1 + J_{a1}^{T}(q_1)\left(m_o J_{o1}(q_1)\ddot{q}_1 + m_o \dot{J}_{o1}(q_1)\dot{q}_1 - m_o g_o + f_2\right) = \\ &\tau_1 + J_{a1}^{T}(q_1) m_o J_{o1}(q_1)\ddot{q}_1 + J_{a1}^{T}(q_1) m_o \dot{J}_{o1}(q_1)\dot{q}_1 - J_{a1}^{T}(q_1) m_o g_o + J_{a1}^{T}(q_1) f_2\,, \end{aligned} \tag{22}$$

or

$$\begin{aligned} \tau_1 + J_{a1}^{T}(q_1) f_2 &= \left(H_1(q_1) - J_{a1}^{T}(q_1) m_o J_{o1}(q_1)\right)\ddot{q}_1 \\ &+ \left(C_1(q_1,\dot{q}_1) + D_1 - J_{a1}^{T}(q_1) m_o \dot{J}_{o1}(q_1)\right)\dot{q}_1 + g_1(q_1) + J_{a1}^{T}(q_1) m_o g_o\,. \end{aligned} \tag{23}$$

By defining

$$H_{T1}(q_1) \triangleq H_1(q_1) - J_{a1}^{T}(q_1) m_o J_{o1}(q_1) \quad (24)$$

$$C_{T1}(q_1, \dot{q}_1) \triangleq C_1(q_1, \dot{q}_1) + D_1 - J_{a1}^{T}(q_1) m_o \dot{J}_{o1}(q_1) \quad (25)$$

$$g_{T1}(q_1) \triangleq g_1(q_1) + J_{a1}^{T}(q_1) m_o g_o, \quad (26)$$

one finally gets

$$H_{T1}(q_1)\ddot{q}_1 + C_{T1}(q_1, \dot{q}_1)\dot{q}_1 + g_{T1}(q_1) = \tau_1 + J_{a1}^{T}(q_1) f_2. \quad (27)$$

In the same fashion, we make the analysis for the robot A255, to get

$$H_{T2}(q_2)\ddot{q}_2 + C_{T2}(q_2, \dot{q}_2)\dot{q}_2 + g_{T2}(q_2) = \tau_2 + J_{a2}^{T}(q_2) f_1, \quad (28)$$

with

$$H_{T2}(q_2) \triangleq H_2(q_2) + J_{a2}^{T}(q_2) m_o J_{o2}(q_2) \quad (29)$$

$$C_{T2}(q_2, \dot{q}_2) \triangleq C_2(q_2, \dot{q}_2) + D_2 + J_{a2}^{T}(q_2) m_o \dot{J}_{o2}(q_2) \quad (30)$$

$$g_{T2}(q_2) \triangleq g_2(q_2) - J_{a2}^{T}(q_2) m_o g_o. \quad (31)$$

The dynamic models in (27)-(28) describe the motion of the entire closed chain, where each individual manipulator represents a subsystem coupled to the other one through kinematic and dynamic constraints.

3.4 Force modeling for cooperative robots

A robot manipulator in free motion does not have geometric constraints; therefore, the dynamic model is described by Ordinary Differential Equations (ODE). When working with constrained motion, there appear holonomic constraints; for this reason, the dynamic model is described by Differential Algebraic Equations (DAE). To simulate contact forces, DAE's must be solved. First of all, from the dynamic model for cooperative robots (1), we obtain

$$\ddot{q}_i = H_i^{-1}(q_i)\left(\tau_i + J_{\varphi_i}^{T}(q_i)\lambda_i - C_i(q_i, \dot{q}_i)\dot{q}_i - D_i\dot{q}_i - g_i(q_i)\right) \quad (32)$$

However, (7)-(9) must hold as well. Substituting the right hand side of (32) into (9) yields

$$\begin{aligned} \ddot{\varphi}_i(q_i) &= J_{\varphi i}(q_i)\left[H_i^{-1}(q_i)\left(\tau_i + J_{\varphi_i}^{T}(q_i)\lambda_i - C_i(q_i, \dot{q}_i)\dot{q}_i - D_i\dot{q}_i - g_i(q_i)\right)\right] \\ &\quad + \dot{J}_{\varphi i}(q_i)\dot{q}_i \\ &= J_{\varphi i}(q_i)H_i^{-1}(q_i)J_{\varphi_i}^{T}(q_i)\lambda_i + \dot{J}_{\varphi i}(q_i)\dot{q}_i \\ &\quad + J_{\varphi i}(q_i)H_i^{-1}(q_i)\left(\tau_i - C_i(q_i, \dot{q}_i)\dot{q}_i - D_i\dot{q}_i - g_i(q_i)\right) \\ &= 0. \end{aligned} \quad (33)$$

From the previous equation we obtain

$$\begin{aligned} \lambda_i &= \left(J_{\varphi i}(q_i)H_i^{-1}(q_i)J_{\varphi_i}^{T}(q_i)\right)^{-1}\left[\ddot{\varphi}_i(q_i) - \dot{J}_{\varphi i}(q_i)\dot{q}_i\right. \\ &\quad \left. - J_{\varphi i}(q_i)H_i^{-1}(q_i)\left(\tau_i - C_i(q_i, \dot{q}_i)\dot{q}_i - D_i\dot{q}_i - g_i(q_i)\right)\right] \end{aligned} \quad (34)$$

The system described by (11), (27)-(28) and (34) could now be simulated as second order differential equations. However, the inclusion of the constraints in the form (34) does not guarantee the convergence of the contact velocity and position constraints to zero. This is because $\ddot{\varphi}_i(q_i) = 0$ represents a double integrator. Thus, any small

difference of $\boldsymbol{\varphi}_i(\boldsymbol{q}_i)$ or $\dot{\boldsymbol{\varphi}}_i(\boldsymbol{q}_i)$ from zero in (7)-(9) will diverge. This problem has been successfully addressed by the constraint stabilization method in the solution of DAE's (Baumgarte 1972).
According to this approach, the constraints are asymptotically stabilized by using

$$\ddot{\boldsymbol{\varphi}}_i(\boldsymbol{q}_i)+2\alpha_i\dot{\boldsymbol{\varphi}}_i(\boldsymbol{q}_i)+\beta_i\boldsymbol{\varphi}_i(\boldsymbol{q}_i)=0\,, \tag{35}$$

instead of $\ddot{\boldsymbol{\varphi}}_i(\boldsymbol{q}_i)=0$. α_i and β_i are chosen appropriately to ensure the fast convergence of both the constraint position $\boldsymbol{\varphi}_i(\boldsymbol{q}_i)$ and velocity constraint $\dot{\boldsymbol{\varphi}}_i(\boldsymbol{q}_i)$ to zero (in case of offset). Equations (11), (27)-(28) and (34)-(35) fully describe the motion of the system to be simulated (Gudiño-Lau & Arteaga 2005).

4. Control with velocity estimation

4.1 Control Law

In this section, a linear filter for the force error and the tracking control problem of a cooperative system of rigid robots are studied. Consider model (1) and define the tracking and observation errors as

$$\tilde{\boldsymbol{q}}_i \triangleq \boldsymbol{q}_i - \boldsymbol{q}_{\mathrm{d}i} \tag{36}$$

$$\boldsymbol{z}_i \triangleq \boldsymbol{q}_i - \hat{\boldsymbol{q}}_i\,, \tag{37}$$

where $\boldsymbol{q}_{\mathrm{d}i}$ is a desired smooth bounded trajectory satisfying constraint (2), and $(\hat{\bullet})$ represents the estimated value of $(\bullet)$. Other error definitions are

$$\Delta\boldsymbol{p}_i \triangleq \boldsymbol{p}_i - \boldsymbol{p}_{\mathrm{d}i} \tag{38}$$

$$\Delta\boldsymbol{\lambda}_i \triangleq \boldsymbol{\lambda}_i - \boldsymbol{\lambda}_{\mathrm{d}i} \tag{39}$$

where $\boldsymbol{p}_{\mathrm{d}i}$ is the desired constrained position which satisfies (6). $\boldsymbol{\lambda}_{\mathrm{d}i}$ is the desired force to be applied by each finger on the constrained surface. Other useful definitions are

$$\dot{\boldsymbol{q}}_{\mathrm{r}i} \triangleq \boldsymbol{Q}_i(\boldsymbol{q}_i)\left(\dot{\boldsymbol{q}}_{\mathrm{d}i} - \Lambda_i(\hat{\boldsymbol{q}}_i - \boldsymbol{q}_{\mathrm{d}i})\right) + \boldsymbol{J}_{\varphi i}^{+}(\boldsymbol{q}_i)\left(\dot{\boldsymbol{p}}_{\mathrm{d}i} - \beta_i\Delta\boldsymbol{p}_i + \bar{\xi}_i\boldsymbol{\phi}_i + \xi_i\Delta\boldsymbol{F}_i\right) \tag{40}$$

$$\begin{aligned}\boldsymbol{s}_i &\triangleq \dot{\boldsymbol{q}}_i - \dot{\boldsymbol{q}}_{\mathrm{r}i}\\ &= \boldsymbol{Q}_i(\boldsymbol{q}_i)\left(\dot{\tilde{\boldsymbol{q}}}_i + \Lambda_i\tilde{\boldsymbol{q}}_i - \Lambda_i\boldsymbol{z}_i\right) + \boldsymbol{J}_{\varphi i}^{+}(\boldsymbol{q}_i)\left(\Delta\dot{\boldsymbol{p}}_i + \beta_i\Delta\boldsymbol{p}_i - \bar{\xi}_i\boldsymbol{\phi}_i - \xi_i\Delta\boldsymbol{F}_i\right).\\ &\triangleq \boldsymbol{s}_{\mathrm{p}i} + \boldsymbol{s}_{\mathrm{f}i}\end{aligned} \tag{41}$$

$$\Delta\boldsymbol{F}_i \triangleq \int_0^t \Delta\boldsymbol{\lambda}_i(\vartheta)\,\mathrm{d}\vartheta\,, \tag{42}$$

where $\Lambda_i = k_i\boldsymbol{I} \in \mathbb{R}^{m_i\times m_i}$ with $k_i > 0$, and $\bar{\xi}_i$, $\xi_i \in \mathbb{R}^{m_i\times m_i}$ are diagonal positive definite matrices, and β_i is a positive constant. To get (41) the equality $\hat{\boldsymbol{q}}_i - \boldsymbol{q}_{\mathrm{d}i} = \tilde{\boldsymbol{q}}_i - \boldsymbol{z}_i$ has been used. Note also that $\boldsymbol{s}_{\mathrm{p}i}$ and $\boldsymbol{s}_{\mathrm{f}i}$ are orthogonal vectors. $\boldsymbol{\phi}_i \in \mathbb{R}^{m_i}$ is the output of the linear filter given by

$$\dot{\boldsymbol{w}}_i = -\boldsymbol{A}_i\boldsymbol{w}_i + \Delta\boldsymbol{\lambda}_i \qquad \boldsymbol{w}_i(0) = 0 \tag{43}$$

$$\boldsymbol{\phi}_i = \boldsymbol{B}_i\boldsymbol{w}_i\,. \tag{44}$$

$\boldsymbol{A}_i$, $\boldsymbol{B}_i \in \mathbb{R}^{m_i\times m_i}$ are diagonal positive definite matrices and $\boldsymbol{w}_i \in \mathbb{R}^{m_i}$ is the state for the filter. Also, we define

$$\zeta_i \triangleq \dot{\boldsymbol{\phi}}_i = -\boldsymbol{B}_i\boldsymbol{A}_i\boldsymbol{w}_i + \boldsymbol{B}_i\Delta\boldsymbol{\lambda}_i = -\boldsymbol{A}_i\boldsymbol{\phi}_i + \boldsymbol{B}_i\Delta\boldsymbol{\lambda}_i\,. \tag{45}$$

Now, let us analyze $\boldsymbol{q}_{ri}$. This quantity is given by

$$\begin{aligned}\ddot{\boldsymbol{q}}_{ri} &\triangleq \boldsymbol{Q}_i(\boldsymbol{q}_i)\left(\ddot{\boldsymbol{q}}_{di} - \Lambda_i\left(\dot{\hat{\boldsymbol{q}}}_i - \dot{\boldsymbol{q}}_{di}\right)\right) + \boldsymbol{J}_{\varphi i}^{+}(\boldsymbol{q}_i)\left(\ddot{\boldsymbol{p}}_{di} - \beta_i(\dot{\boldsymbol{p}}_i - \dot{\boldsymbol{p}}_{di}) + \bar{\xi}_i\zeta_i + \xi_i\Delta\lambda_i\right) \\ &+ \dot{\boldsymbol{Q}}_i(\boldsymbol{q}_i)\left(\dot{\boldsymbol{q}}_{di} - \Lambda_i(\hat{\boldsymbol{q}}_i - \boldsymbol{q}_{di})\right) + \dot{\boldsymbol{J}}_{\varphi i}^{+}(\boldsymbol{q}_i)\left(\dot{\boldsymbol{p}}_{di} - \beta_i\Delta\boldsymbol{p}_i + \bar{\xi}_i\boldsymbol{\phi}_i + \xi_i\Delta F_i\right).\end{aligned} \tag{46}$$

As it will be shown later, $\ddot{\boldsymbol{q}}_{ri}$ is necessary to implement the controller and the observer. However, this quantity is not available since $\dot{\boldsymbol{q}}_i$ is not measurable. In order to overcome this drawback, let us consider $\boldsymbol{Q}_i(\boldsymbol{q}_i) \in \mathbb{R}^{n_i \times n_i}$. Then you have

$$\dot{\boldsymbol{Q}}_i(\boldsymbol{q}_i) = \begin{bmatrix} \dfrac{\partial a_{11}(\boldsymbol{q}_i)}{\partial \boldsymbol{q}_i}\dot{\boldsymbol{q}}_i & \cdots & \dfrac{\partial a_{1n_i}(\boldsymbol{q}_i)}{\partial \boldsymbol{q}_i}\dot{\boldsymbol{q}}_i \\ \vdots & \ddots & \vdots \\ \dfrac{\partial a_{n_i1}(\boldsymbol{q}_i)}{\partial \boldsymbol{q}_i}\dot{\boldsymbol{q}}_i & \cdots & \dfrac{\partial a_{n_in_i}(\boldsymbol{q}_i)}{\partial \boldsymbol{q}_i}\dot{\boldsymbol{q}}_i \end{bmatrix}, \tag{47}$$

where $a_{\alpha\beta}$ is the $\alpha\beta$ element of $\boldsymbol{Q}_i(\boldsymbol{q}_i)$. Based on (47), consider the following definition

$$\dot{\hat{\boldsymbol{Q}}}_i(\boldsymbol{q}_i) \triangleq \begin{bmatrix} \dfrac{\partial a_{11}(\boldsymbol{q}_i)}{\partial \boldsymbol{q}_i}\dot{\boldsymbol{q}}_{oi} & \cdots & \dfrac{\partial a_{1n_i}(\boldsymbol{q}_i)}{\partial \boldsymbol{q}_i}\dot{\boldsymbol{q}}_{oi} \\ \vdots & \ddots & \vdots \\ \dfrac{\partial a_{n_i1}(\boldsymbol{q}_i)}{\partial \boldsymbol{q}_i}\dot{\boldsymbol{q}}_{oi} & \cdots & \dfrac{\partial a_{n_in_i}(\boldsymbol{q}_i)}{\partial \boldsymbol{q}_i}\dot{\boldsymbol{q}}_{oi} \end{bmatrix}, \tag{48}$$

with

$$\dot{\boldsymbol{q}}_{oi} \triangleq \dot{\hat{\boldsymbol{q}}}_i - \Lambda_i z_i. \tag{49}$$

Then, one can compute

$$\dot{\tilde{\boldsymbol{Q}}}_i(\boldsymbol{r}_i) \triangleq \dot{\boldsymbol{Q}}_i(\boldsymbol{q}_i) - \dot{\hat{\boldsymbol{Q}}}_i(\dot{\boldsymbol{q}}_{oi}) = \begin{bmatrix} \dfrac{\partial a_{11}(\boldsymbol{q}_i)}{\partial \boldsymbol{q}_i}\boldsymbol{r}_i & \cdots & \dfrac{\partial a_{1n_i}(\boldsymbol{q}_i)}{\partial \boldsymbol{q}_i}\boldsymbol{r}_i \\ \vdots & \ddots & \vdots \\ \dfrac{\partial a_{n_i1}(\boldsymbol{q}_i)}{\partial \boldsymbol{q}_i}\boldsymbol{r}_i & \cdots & \dfrac{\partial a_{n_in_i}(\boldsymbol{q}_i)}{\partial \boldsymbol{q}_i}\boldsymbol{r}_i \end{bmatrix}, \tag{50}$$

where

$$\boldsymbol{r}_i \triangleq \dot{\boldsymbol{q}}_i - \dot{\boldsymbol{q}}_{oi} = \dot{z}_i + \Lambda_i z_i. \tag{51}$$

In view of (48), we propose the following substitution for $\ddot{\boldsymbol{q}}_{ri}$

$$\begin{aligned}\ddot{\hat{\boldsymbol{q}}}_{ri} &\triangleq \boldsymbol{Q}_i(\boldsymbol{q}_i)\left(\ddot{\boldsymbol{q}}_{di} - \Lambda_i\left(\dot{\hat{\boldsymbol{q}}}_i - \dot{\boldsymbol{q}}_{di}\right)\right) + \boldsymbol{J}_{\varphi i}^{+}(\boldsymbol{q}_i)\left(\ddot{\boldsymbol{p}}_{di} - \beta_i(\dot{\boldsymbol{p}}_i - \dot{\boldsymbol{p}}_{di}) + \bar{\xi}_i\zeta_i + \xi_i\Delta\lambda_i\right) \\ &+ \dot{\boldsymbol{Q}}_i(\boldsymbol{q}_i)\left(\dot{\boldsymbol{q}}_{di} - \Lambda_i(\hat{\boldsymbol{q}}_i - \boldsymbol{q}_{di})\right) + \dot{\hat{\boldsymbol{J}}}_{\varphi i}^{+}(\boldsymbol{q}_i)\left(\dot{\boldsymbol{p}}_{di} - \beta_i\Delta\boldsymbol{p}_i + \bar{\xi}_i\boldsymbol{\phi}_i + \xi_i\Delta F_i\right),\end{aligned} \tag{52}$$

where $\dot{\hat{\boldsymbol{J}}}_{\varphi i}^{+}(\boldsymbol{q}_i)$ is defined in the very same fashion as $\dot{\hat{\boldsymbol{Q}}}_i(\boldsymbol{q}_i)$ in (48). Note that $\dot{\boldsymbol{p}}_i$ is still used since this value is known from (6). After some manipulation, it is possible to get

$$\ddot{\tilde{\boldsymbol{q}}}_{ri} = \ddot{\boldsymbol{q}}_{ri} + \boldsymbol{e}_i(\boldsymbol{r}_i), \tag{53}$$

where

$$e_i(r_i) \triangleq -\dot{\bar{Q}}_i(q_i)\left(\dot{q}_{di} - \Lambda_i\tilde{q}_i + \Lambda_i z_i\right) - \dot{\bar{J}}_{\varphi i}^{+}(q_i)\left(\dot{p}_{di} - \beta_i\Delta p_i + \bar{\xi}_i\phi_i + \xi_i\Delta F_i\right) \tag{54}$$

The proposed controller is then given for each single input by

$$\begin{aligned}\tau_i \;\triangleq\; & H_i(q_i)\ddot{q}_{ri} + C_i(q_i,\dot{q}_{ri})\dot{q}_{ri} + D_i\dot{q}_{ri} + g_i(q_i) \\ & - K_{Ri}(\dot{q}_{oi} - \dot{q}_{ri}) - J_{\varphi i}^{\mathrm{T}}(q_i)\left(\lambda_{di} + B_i^{-1}\zeta_i - K_{Fi}\Delta F_i\right),\end{aligned} \tag{55}$$

where $K_{Ri} \in \mathbb{R}^{n_i \times n_i}$, $K_{Fi} \in \mathbb{R}^{m_i \times m_i}$ are diagonal positive definite matrices. Note that from (41) and (51) it is $\dot{q}_{oi} - \dot{q}_{ri} = s_i - r_i$. Thus, from (53) one gets

$$\begin{aligned}\tau_i \;=\; & H_i(q_i)\left(\ddot{q}_{ri} + e_i(r_i)\right) + C_i(q_i,\dot{q}_{ri})\dot{q}_{ri} + D_i\dot{q}_{ri} + g_i(q_i) \\ & - K_{Ri}(s_i - r_i) - J_{\varphi i}^{\mathrm{T}}(q_i)\left(\lambda_{di} + B_i^{-1}\zeta_i - K_{Fi}\Delta F_i\right).\end{aligned} \tag{56}$$

By substituting (56) into (1), the closed loop dynamics becomes

$$\begin{aligned}H_i(q_i)\dot{s}_i \;=\; & -C_i(q_i,\dot{q}_i)s_i - K_{DRi}s_i + K_{Ri}r_i \\ & + J_{\varphi i}^{\mathrm{T}}(q_i)\left(B_i^{-1}A_i\phi_i + K_{Fi}\Delta F_i\right) - C_i(q_i,\dot{q}_{ri})s_i + H_i(q_i)e_i(r_i)\end{aligned} \tag{57}$$

after some manipulation, where $K_{DRi} \triangleq K_{Ri} + D_i$. In order to get (57), Property 3.3 has been used.

4.2 Observer definition

The proposed dynamics of the observer is given by

$$\dot{\hat{q}}_i = \dot{\hat{q}}_{oi} + \Lambda_i z_i + k_{di} z_i \tag{58}$$

$$\ddot{\hat{q}}_{oi} = \ddot{\hat{q}}_{ri} + k_{di}\Lambda_i z_i, \tag{59}$$

where k_{di} is a positive constant. This observer is simpler than the one given in (Gudiño-Lau *et al.* 2004), where the inverse of the inertia matrix and force measurements are required. Since from (58) you have $\ddot{\hat{q}}_{oi} = \ddot{\hat{q}}_i - \Lambda_i\dot{z}_i - k_{di}\dot{z}_i$, (59) becomes

$$\dot{s}_i = \dot{r}_i + k_{di}r_i + e_i(r_i), \tag{60}$$

in view of (53). By multiplying both sides of (60) by $H_i(q_i)$, and by taking into account (57), one gets

$$\begin{aligned}H_i(q_i)\dot{r}_i \;=\; & -H_{rdi}r_i - C_i(q_i,\dot{q}_i)s_i - C_i(q_i,\dot{q}_{ri})s_i - K_{DRi}s_i \\ & + J_{\varphi i}^{\mathrm{T}}(q_i)\left(B_i^{-1}A_i\phi_i + K_{Fi}\Delta F_i\right),\end{aligned} \tag{61}$$

where $H_{rdi} \triangleq k_{di}H_i(q_i) - K_{Ri}$. Finally, by using Property 3.3 again and some manipulation, it is

$$\begin{aligned}H_i(q_i)\dot{r}_i \;=\; & -C_i(q_i,\dot{q}_i)r_i - H_{rdi}r_i + C_i(q_i,s_i + \dot{q}_{ri})r_i - K_{DRi}s_i \\ & - C_i(q_i,s_i + 2\dot{q}_{ri})s_i + J_{\varphi i}^{\mathrm{T}}(q_i)\left(B_i^{-1}A_i\phi_i + K_{Fi}\Delta F_i\right).\end{aligned} \tag{62}$$

Now, let us define

$$x_i \triangleq \begin{bmatrix} s_i^{\mathrm{T}} & r_i^{\mathrm{T}} & \Delta F_i^{\mathrm{T}} & \phi_i^{\mathrm{T}} \end{bmatrix}^{\mathrm{T}}, \tag{63}$$

as state for (42), (45), (57) and (62). The main idea of the control-observer design is to show that whenever $\|x_i\|$ tends to zero, the tracking errors $\tilde{q}_i$, $\dot{\tilde{q}}_i$, Δp_i, $\Delta\dot{p}_i$ and $\Delta\lambda_i$ and the

observation errors $\boldsymbol{z}_i$ and $\dot{\boldsymbol{z}}_i$ will do it as well. From (51), this is rather obvious for $\boldsymbol{z}_i$ and $\dot{\boldsymbol{z}}_i$. However, it is not clear for the other variables. The following lemma shows that this is indeed the case under some conditions.

Lemma 4.1 If $\boldsymbol{x}_i$ is bounded by $\boldsymbol{x}_{\max i}$ and tends to zero, then the following facts hold:

a) $\Delta\boldsymbol{p}_i$ *and* $\Delta\dot{\boldsymbol{p}}_i$ *remain bounded and tend to zero*

b) $\tilde{\boldsymbol{q}}_i$ *and* $\dot{\tilde{\boldsymbol{q}}}_i$ *remain bounded. Furthermore, if the bound* $\boldsymbol{x}_{\max i}$ *for* $\|\boldsymbol{x}_i\|$ *is chosen small enough so as to guarantee that* $\|\tilde{\boldsymbol{q}}_i\| \le \eta_i$ *for all t, with* η_i *a positive and small enough constant, then both* $\tilde{\boldsymbol{q}}_i$ *and* $\dot{\tilde{\boldsymbol{q}}}_i$ *will tend to zero as well.*

c) If, in addition, the velocity vector $\dot{\boldsymbol{q}}_i$ *is bounded, then* $\Delta\boldsymbol{\lambda}_i$ *will remain bounded and tend to zero.* Δ

The proof of Lemma 4.1 can be found in Appendix B. It is interesting to note that, if $\|\boldsymbol{x}_i\|$ is bounded by $\boldsymbol{x}_{\max i}$, then it is always possible to find a bound for $\boldsymbol{e}_i(\boldsymbol{r}_i)$ in (54) which satisfies

$$\|\boldsymbol{e}_i(\boldsymbol{r}_i)\| \le M_{ei}(\boldsymbol{x}_{\max i})\|\boldsymbol{r}_i\| < \infty . \tag{64}$$

Consider now the following function

$$V_i(\boldsymbol{x}_i) = \frac{1}{2}\boldsymbol{x}_i^{\mathrm{T}}\boldsymbol{M}_i\boldsymbol{x}_i , \tag{65}$$

where $\boldsymbol{M}_i \triangleq \text{block diag}\{\boldsymbol{H}_i(\boldsymbol{q}_i),\ \boldsymbol{H}_i(\boldsymbol{q}_i),\ \boldsymbol{R}_i\}$, and

$$\boldsymbol{R}_i \triangleq \begin{bmatrix} \boldsymbol{N}_i\boldsymbol{B}_i^{-1} & -\boldsymbol{N}_i \\ -\boldsymbol{N}_i & \boldsymbol{N}_i\boldsymbol{B}_i \end{bmatrix}, \tag{66}$$

with $\boldsymbol{N}_i \triangleq \left(\boldsymbol{\xi}_i\boldsymbol{B}_i^{-1}\boldsymbol{A}_i + \bar{\boldsymbol{\xi}}_i\boldsymbol{K}_{Fi}\right)\boldsymbol{A}_i^{-1}$. In Appendix C it is shown that $V_i(\boldsymbol{x}_i)$ is a positive definite function. Suppose that one may find a region

$$\mathbb{D}_i = \{\boldsymbol{x}_i :\ \|\boldsymbol{x}_i\| \le \boldsymbol{x}_{\max i}\}, \tag{67}$$

so that for all time $\dot{V}_i(\boldsymbol{x}_i) \le 0$ with $\dot{V}_i(\boldsymbol{x}_i) = 0$ if and only if $\boldsymbol{x}_i = \boldsymbol{0}$. If $\boldsymbol{x}_{\max i}$ is small enough in the sense of Lemma 4.1, then from the former discussion one can conclude the convergence to zero of all error signals. The following theorem establishes the conditions for the controller-observer parameters to guarantee this.

Teorema 4.1 *Consider the cooperative system dynamics given by (1), (2) and (6), in closed loop with the filter (43)-(45), the control law (55) and the observer (58)-(59), where* $\boldsymbol{q}_{\mathrm{d}i}$ *and* $\boldsymbol{p}_{\mathrm{d}i}$ *are the desired bounded joint and constrained positions, whose derivatives* $\dot{\boldsymbol{q}}_{\mathrm{d}i}$, $\ddot{\boldsymbol{q}}_{\mathrm{d}i}$, $\dot{\boldsymbol{p}}_{\mathrm{d}i}$, *and* $\ddot{\boldsymbol{p}}_{\mathrm{d}i}$ *are also bounded, and they all satisfy constraint (6). Consider also l given regions defined by (67) for each subsystem, where the bounds* $\boldsymbol{x}_{\max i}$, $i = 1,\ldots,l$, *are chosen according to*

$$\boldsymbol{x}_{\max i} \le \frac{\eta_i\alpha_i}{\left(1 + c_{0i}\left(\lambda_{\max}\left(\bar{\boldsymbol{\xi}}_i\right) + \lambda_{\max}\left(\boldsymbol{\xi}_i\right)\right) + \sqrt{n_i}\right)} \tag{68}$$

with α_i *defined in Appendix B. Then, every dynamic and error signal remains bounded and asymptotic stability of tracking, observation and force errors arise, i. e.*

$$\lim_{t\to\infty}\tilde{\boldsymbol{q}}_i = \mathbf{0} \quad \lim_{t\to\infty}\dot{\tilde{\boldsymbol{q}}}_i = \mathbf{0} \quad \lim_{t\to\infty}\boldsymbol{z}_i = \mathbf{0} \quad \lim_{t\to\infty}\dot{\boldsymbol{z}}_i = \mathbf{0} \quad \lim_{t\to\infty}\Delta\boldsymbol{\lambda}_i = \mathbf{0}, \tag{69}$$

if the following conditions are satisfied

$$\lambda_{\min}\left(\boldsymbol{K}_{\mathrm{R}i}\right) \geq \mu_{1i} + 1 + \delta_i \tag{70}$$

$$k_{\mathrm{d}i} \geq \frac{\lambda_{\max}\left(\boldsymbol{K}_{\mathrm{R}i}\right) + w_i}{\lambda_{\mathrm{h}i}} \tag{71}$$

$$\lambda_{\min}\left(\boldsymbol{E}_i\right) \geq \delta_i + 1 \tag{72}$$

$$\lambda_{\min}\left(\boldsymbol{\xi}_i\boldsymbol{K}_{\mathrm{F}i}\right) \geq \delta_i + 1, \tag{73}$$

where $w_i = \mu_{2i} + \frac{1}{4}\left(\lambda_{\mathrm{D}i} + \mu_{3i} + \mu_{4i}\right)^2 + \delta_i + \frac{1}{4}c_{1i}^2 a_i^2 b_i^2 + \frac{1}{4}c_{1i}^2\lambda_{\max}^2\left(\boldsymbol{K}_{\mathrm{F}i}\right)$, $\boldsymbol{E}_i = \bar{\boldsymbol{\xi}}_i\boldsymbol{B}_i^{-1}\boldsymbol{A}_i + \boldsymbol{\xi}_i\boldsymbol{B}_i^{-2}\boldsymbol{A}_i + \bar{\boldsymbol{\xi}}_i\boldsymbol{K}_{\mathrm{F}i}\boldsymbol{B}_i^{-1}$, δ_i *a positive constant* and μ_{1i}, μ_{2i}, μ_{3i}, μ_{4i} and $\lambda_{\mathrm{D}i}$ *defined in Appendix D.* Δ

The proof of the Theorem 4.1 can be found in Appendix D

Remark 4.1 *The result of Theorem 4.1 is only local. Also, it is rather difficult to find analytically a region of attraction, but it should be noticed that it {\it cannot} be made arbitrarily large. This is to guarantee the convergence to zero of the tracking errors* $\tilde{\boldsymbol{q}}_i$ *and* $\dot{\tilde{\boldsymbol{q}}}_i$*. However, this does not represent a serious drawback since for grasping purposes it is usual to give smooth trajectories with zero initial position errors. On the other hand, it is worthy pointing out that a controller-observer scheme is implemented for every robot separately, while only the knowledge of each constraint of the form (2) is required.* Δ.

5. Simulation and Experimental Results

In this section, some simulation results are presented. To test the accuracy of the modeling approach, experimental results are carried out as well. To protect the manipulators of the cooperative system again possible damages, the position/force control law (55) has been used for validation purposes, the motors dynamics has to be taken into account. For the object equation of motion given in (10), it is $\boldsymbol{m}_{\mathrm{o}} = m_{\mathrm{obj}}\boldsymbol{I}$, $m_{\mathrm{obj}} = 0.400\mathrm{kg}$, and $\boldsymbol{g}_{\mathrm{o}}^{\mathrm{T}} = \left\{g_x \quad g_y \quad g_z\right\} = \left\{0 \quad 0 \quad -9.81\mathrm{m/s}^2\right\}$. The object dimensions are $0.15\mathrm{m}\times 0.15\mathrm{m}\times 0.311\mathrm{m}$. In (35) one has $\alpha_i = 10$ and $\beta_i = 100$. The robots models are given in Appendix A.

The palm frame of the whole system is at the base of the robot A465, with its ***x***-axis pointing towards the other manipulator. The task consists in lifting the object and pushing with a desired force, so that the constraints in Cartesian coordinates are simply given by

$$\varphi_i = x_i - b_i = 0, \tag{74}$$

for ***i*** = 1, 2 and b_i a positive constant. The desired trajectories are given by

$$x_{d1} = 0.554\,[\mathrm{m}] \qquad x_{d2} = 0.865\,[\mathrm{m}] \tag{75}$$

$$y_{d1,2} = 0.05\sin(w(t-t_i))\,[\mathrm{m}] \tag{76}$$

$$z_{d1,2} = (0.635 + 0.05\cos(w(t-t_i)) - 0.05)\,[\mathrm{m}] \tag{77}$$

Note that the inverse kinematics of the manipulators has to be employed to compute $\boldsymbol{q}_{di}$. These trajectories are valid from an initial time $t_i = 10\mathrm{s}$ to a final time $t_f = 70\mathrm{s}$. Before t_i and after t_f the robots are in free motion. w is a fifth order polynomial designed to satisfy $w(t_i) = w(t_f) = 0$. The derivatives of w are also zero at t_i and t_f. By choosing (75)-(77), the robots will make a circle in the y-z plane. The only difference between the trajectories for robots A465 and A255 is the width of the object. Also, no force control is carried out until the manipulators are in the initial position to hold the object, at (0.554,0,0.510)[m] for the first manipulator and (0.865,0,0.510)[m] for the second one. The desired pushing forces are then given from $t = t_i = 10\mathrm{s}$ to $t = t_f = 70\mathrm{s}$ by.

$$f_{dx1,2} = 15(t-t_i)/10[\mathrm{N}] \qquad t_i\mathrm{s} \le t < 20\mathrm{s} \tag{75}$$

$$f_{dx1,2} = 15 + 5\sin(3\pi(t-20)/40[\mathrm{N}] \qquad 20 \le t < 60\mathrm{s} \tag{76}$$

$$f_{dx1,2} = 15 - 7.5(t-60)/10[\mathrm{N}] \qquad 60 \le t < t_f\mathrm{s} \tag{77}$$

and $f_{dy1,2} = f_{dz1,2} = 0[\mathrm{N}]$. Note that, for simplicity, the desired forces are expressed in the base coordinate frame of each robot.

The controller has also been digitalized for the simulation. The experiment lasts 80s. The object is held at t=10s. Before, the robots are in free movement and the control law (55) and the observer (58)-(59) are used with the force part set to zero (*i. e.* $\boldsymbol{Q}_i = \boldsymbol{I}$ and $\boldsymbol{J}_{\varphi i} = \boldsymbol{0}$. It is rather easy to prove that this scheme is stable for unconstrained motion. From t=10s to t=70s it is switched on, *i. e.*, the complete control-observer force scheme is employed only during this period of time. From t=70s to t=80s the robots go back to their initial positions in free motion. From t=10s to t=15s they begin pushing at their initial positions to hold the object, and from t=15s to t=20s they lift it to the position where the circle will be made. From t=20s to t=60s this is done while the desired force is changed for a sinus signal, as can be seen in Figure 6. Note that our purpose is to show that simulation results of the constrained system are acceptable by using the approach described in Section 3. For this reason, the desired forces (or positions) are not shown. Only the real and simulated signals are presented. As can be seen, there is a good match. Of course, simulation results are free of noise. Note also that, since we have not proposed any special method to simulate the moment when the object is held, *i. e.*, when the robots change from free to constrained motion, there is a peak at t=10s in the simulation. From t=60s to t=65s the object is put down on the table and from t=65s to t=70s, the robots diminish pushing. Figure 4 shows the simulation and experimental results of the joint coordinates, while Figure 5 shows the results in Cartesian coordinates. As can be appreciated, the results are good in both cases. On the other hand, the Figure 7 and 8 show only the experimental results, for demonstrate the accuracy of the controller-observer scheme. The Figure 7 show the observation error, as can be appreciated, they are pretty. Finally, Figure 8 show the input voltages. In can observed that there are not saturation problems. This demonstrates the efficacy of designing a decentralized controller.

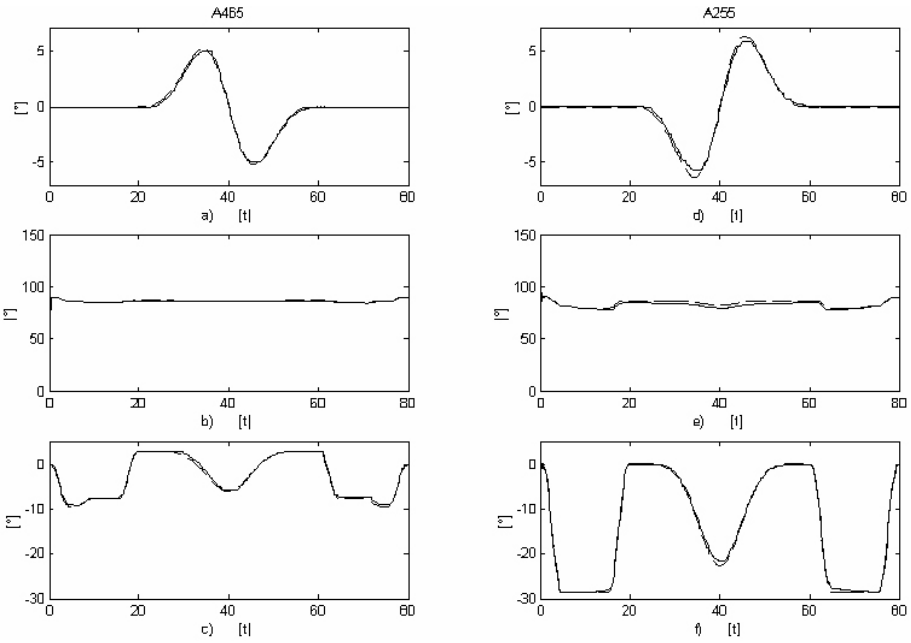

Fig. 4. Tracking in joint coordinates. a) q_{11}. b) q_{12}. c) q_{13}. d) q_{21}. e) q_{22}. f) q_{23}. ----- experiment - - - simulation.

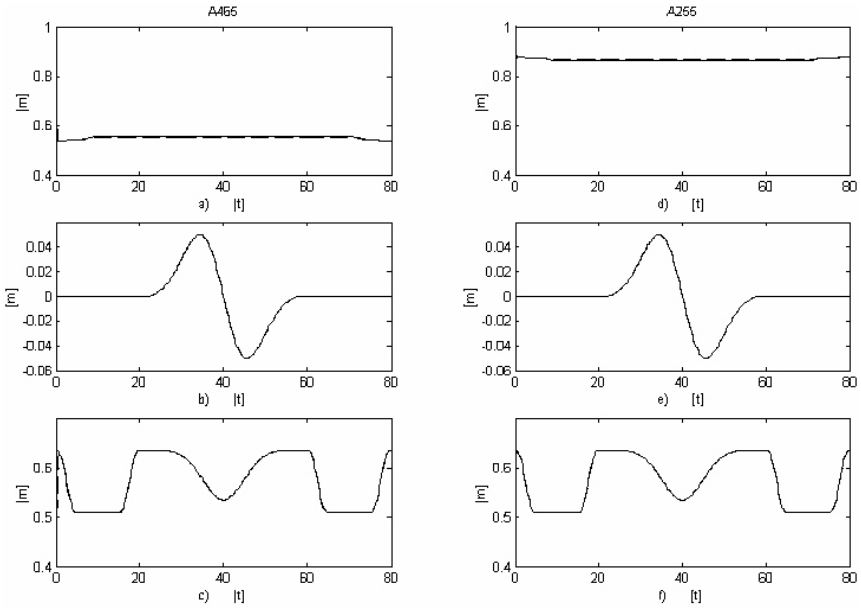

Fig. 5. Tracking in Cartesian coordinates. a) x_1. b) y_1. c) z_1. d) x_2. e) y_2. f) z_2. ----- experiment - - - simulation.

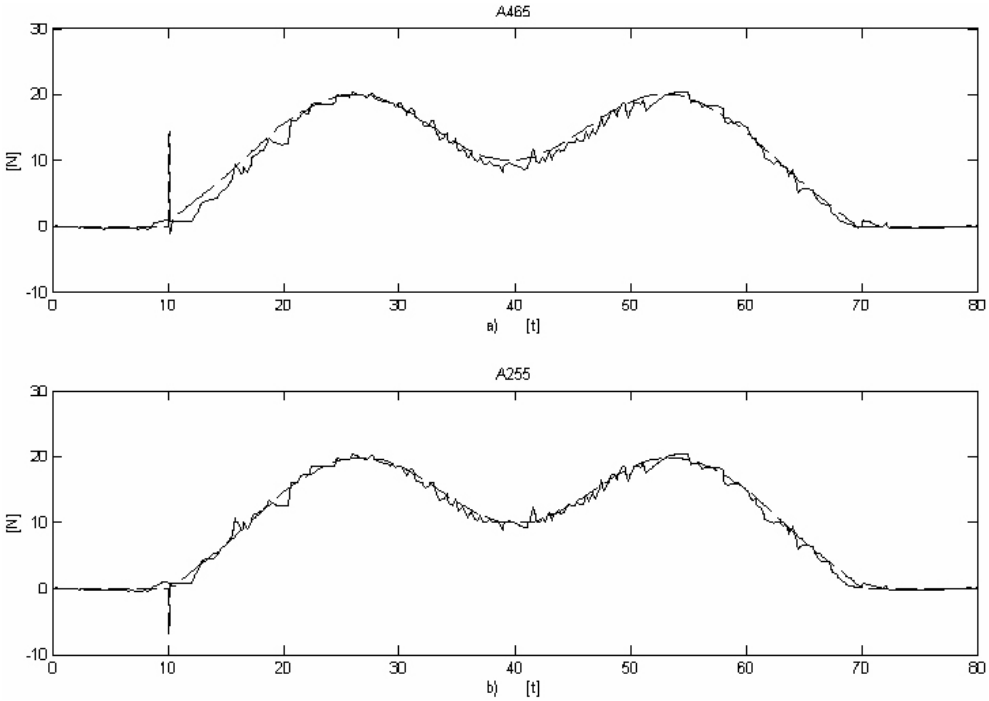

Fig. 6. Force measurements. a) λ_1. b) λ_2 ----- experiment - - - simulation.

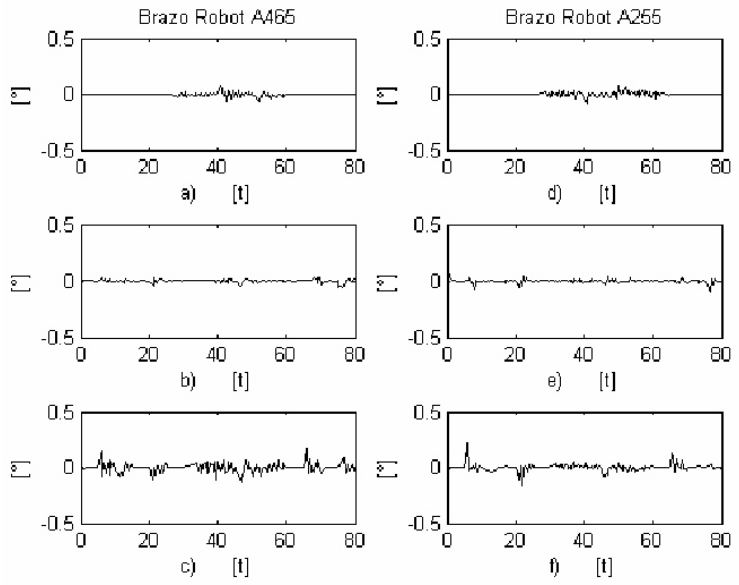

Fig. 7. Observation errors. a) z_{11}. b) z_{12}. c) z_{13}. d) z_{21}. e) z_{22}. f) z_{23}. --- experiment - - - simulation.

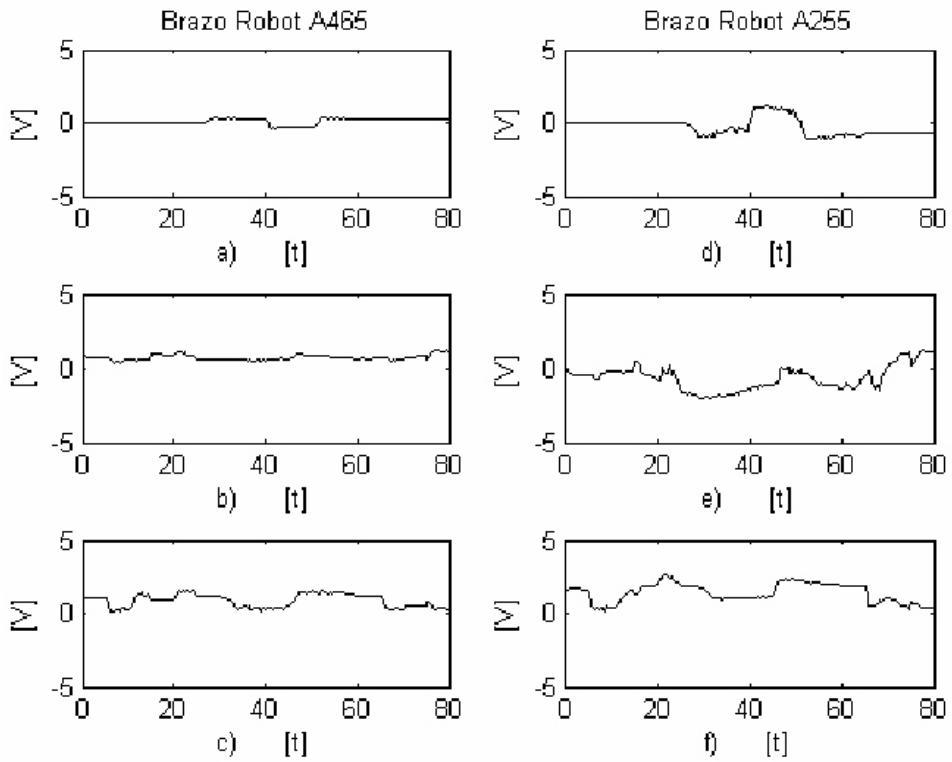

Fig. 8. Input voltages. a) v_{11}. b) v_{12}. c) v_{13}. d) v_{21}. e) v_{22}. f) v_{23}. ----- experiment - - - simulation.

6. Conclusions

In this chapter, we developed the model for two cooperative industrial robots holding a rigid object without friction. The dynamic model for the manipulators is obtained independently from each other with the Lagrangian approach. Once the robots are holding the object, their joint variables are kinematically and dynamically coupled. These coupling equations are combined with the dynamic model of the object to obtain a mathematical description for the cooperative system.

Besides, the tracking control problem for cooperative robots without velocity measurements is considered. The control law is a decentralized approach which takes into account motion constraints rather than the held object dynamics. By assuming that fingers dynamics are well known and that contact forces measurements are available, a linear observer for each finger is proposed which does not require any knowledge of the robots dynamics. Despite the fact that the stability analysis is complex, the controller and specially the observer are not.

Some experiments and simulations have been carried out to test the theoretical results. The overall outcome of the mathematical model compared with the real system can be considered good, which validates the approach used.